CHEMISTRY
A EUROPEAN JOURNAL

FULL PAPER

DOI: 10.1002/chem.201200317

Anion-Induced Shuttling of a Naphthalimide Triazolium Rotaxane

Graeme T. Spence,[a] Mateusz B. Pitak,[b] and Paul D. Beer*[a]

Abstract: The anion-templated synthesis of a rotaxane structure, incorporating the new naphthalimide triazolium motif, is described and the interlocked host shown to exhibit selective, uni-directional, anion-induced shuttling. Initial pseudorotaxane investigations demonstrate the ability of a naphthalimide triazolium threading component to form interpenetrated assemblies with counter-anion-dependent co-conformations. ^{1}H NMR studies reveal that the shuttling behaviour of the analogous rotaxane host system is controlled by selective anion binding and by the nature of the solvent conditions. Complete macrocycle translocation only occurs upon the recognition of the smaller halide anions (chloride and bromide). The rotaxane solid-state crystal structure in the presence of chloride is in agreement with the solution-phase co-conformation. The sensitivity of the axle naphthalimide absorbance band to the position of the macrocycle component within the interlocked structure enabled the molecular motion to be observed by UV/Vis spectroscopy, and the chloride-induced shuttling of the rotaxane was reversed upon silver hexafluorophosphate addition.

Keywords: anions · molecular motion · molecular recognition · rotaxanes · template synthesis

Introduction

The ability of mechanically interlocked molecules to undergo controlled, reversible molecular motion through changes in the relative positions of their constituent parts is receiving an ever increasing amount of interest due to the promise of potential nano-technological applications as molecular switches and machines.[1] However, despite the recent advances in anion supramolecular chemistry,[2] there are still relatively few examples of such interlocked systems being mediated by anions as an external stimulus;[3–6] and of these, only a small number have been shown to display selectivity between different coordinating anions.[4,5]

A key development in molecular machine-like devices is the ability to detect molecular motion through optical or electrochemical signalling. Of those systems induced by the addition of coordinating anions, only Smith's chloride-selective squaraine rotaxane display an associated signalling response,[4] whereby an increase in fluorescence emission is observed upon macrocycle translocation from the central station to one of two triazole groups of the axle. In other, more general types of anion-induced molecular motion, UV/Vis spectroscopy has also been effectively employed as a signalling method.[6,7] In these systems, co-conformational changes were driven either by a change in the non-coordinating counter anion,[6] or by the photo-induced creation of a radical naphthalimide anion within the rotaxane structure.[7]

We report herein the synthesis of a rotaxane capable of controlled, reversible shuttling induced by the addition of coordinating anions (Figure 1). The interlocked structure contains the new naphthalimide triazolium motif within the axle component, and was constructed by using an anion-templation synthetic strategy.[8,9] Molecular motion is driven by binding of an anion in the rotaxane-host cavity, as evidenced by ^{1}H NMR spectroscopy. Importantly, selectivity both in anion binding and the extent of uni-directional macrocycle translocation was observed. In addition, the co-conformational changes exhibited by the rotaxane were found to perturb the absorbance band of the naphthlamide triazolium axle sufficiently for the shuttling process to be signalled and monitored by changes in the rotaxane's UV/Vis spectrum.

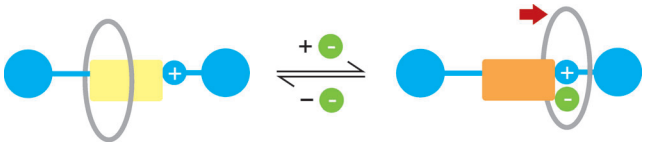

Figure 1. Schematic representation of the anion-induced shuttling behaviour exhibited by a naphthalimide triazolium rotaxane.

Results and Discussion

Pseudorotaxane investigations: To probe the potential of the naphthalimide triazolium motif to form interpenetrative

[a] G. T. Spence, Prof. P. D. Beer
Chemistry Research Laboratory, Department of Chemistry
University of Oxford, Mansfield Road, Oxford, OX1 3TA (UK)
Fax: (+44) 1865-272690
E-mail: paul.beer@chem.ox.ac.uk

[b] Dr. M. B. Pitak
National Crystallography Service, School of Chemistry,
University of Southampton, Highfield Campus
Southampton, SO17 1BJ (UK)

Supporting information for this article is available on the WWW under http://dx.doi.org/10.1002/chem.201200317.

and interlocked assemblies capable of anion-induced, controlled molecular motion, pseudorotaxane studies were carried out initially with thread **1**·BF_4 (prepared as detailed in the Supporting Information) and macrocycle **2**[10] (Figure 2). The naphthalimide motif is intrinsically electron-deficient and further polarized in **1**·BF_4 by the direct attachment of a positively charged triazolium group, which can bind anions through C–H hydrogen bonding.[9] Macrocycle **2** contains an isophthalamide anion binding cleft, containing C–H and N–H hydrogen-bond donors, and electron-rich hydroquinone groups.

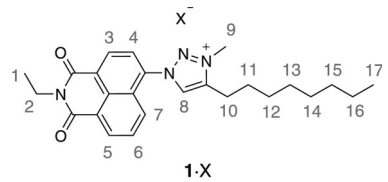

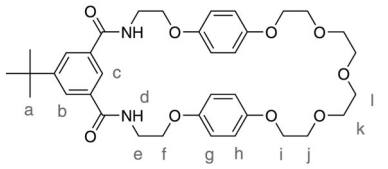

Figure 2. Naphthalimide thread **1**·X and isophthalamide macrocycle **2** used in pseudorotaxane investigations.

These components were designed to undergo interpenetrative assembly due to strong π-donor–π-acceptor interactions between the electron-deficient naphthalimide thread and electron-rich hydroquinone groups of the macrocycle, with cooperative hydrogen bonding to an anion also possible through both the triazolium thread and macrocycle isophthalamide binding motifs. Thus pseudorotaxane co-conformational changes between thread **1**·BF_4 and macrocycle **2** may be controlled by the presence, or absence, of a coordinating anion.

The addition of one equivalent of **1**·BF_4 to macrocycle **2** in $CDCl_3$ was monitored by ^{1}H NMR spectroscopy (Scheme 1 and Figure 3a and b). Pseudorotaxane formation was indicated by a significant upfield shift of macrocycle hydroquinone protons g and h ($\Delta\delta = -0.51$ ppm), due to the highly favourable π-donor–π-acceptor interactions with the electron-deficient naphthalimide thread. In addition, hydrogen-bonding interactions between the imide carbonyl groups of **1**·BF_4 and the macrocycle amide groups resulted in downfield shifts in macrocycle protons c and d. These complementary donor–acceptor and hydrogen-bonding interactions indicate that macrocycle **2** resides directly over the naphthalimide group of thread **1**·BF_4 in the pseudorotaxane assembly, as shown in Scheme 1.

Subsequent addition of one equivalent of tetrabutylammonium (TBA) chloride to **1·2**·BF_4 resulted in a significant change in pseudorotaxane co-conformation, with the macrocycle moving over to the triazolium component of the thread (Scheme 1). Cooperative hydrogen bonding to the halide anion by the macrocycle isophthalamide cleft and thread triazolium group is indicated by downfield shifts in triazolium proton 8 and macrocycle protons c and d (Figure 3c). The hydroquinone protons shift downfield from their position in **1·2**·BF_4 ($\Delta\delta = 0.16$ ppm), due to the reduced shielding effect of the triazolium group in this co-conformation, compared with the larger naphthalimide group, and are split in the presence of the halide anion.

The respective interpenetrated co-conformational nature of assemblies **1·2**·BF_4 and **1·2**·Cl was confirmed by 2D ^{1}H NMR ROESY spectroscopy. A large number of couplings between protons of the macrocycle and the thread are observed for both pseudorotaxane co-conformations, with the spectra and couplings shown in the Supporting Information (Figure S4–S5).

To quantify the stabilities of these two assemblies, ^{1}H NMR pseudorotaxane titrations were carried out in $CDCl_3$. Both **1**·BF_4 and **1**·Cl (prepared by anion exchange detailed in Scheme S1 in the Supporting Information), were titrated into solutions of macrocycle **2** and the signals corresponding to the hydroquinone protons g and h monitored throughout each titration (see Supporting Information, Figure S8). Stability constants were obtained by WinEQNMR2[11] analysis, which gave values of 829(30) M^{-1}

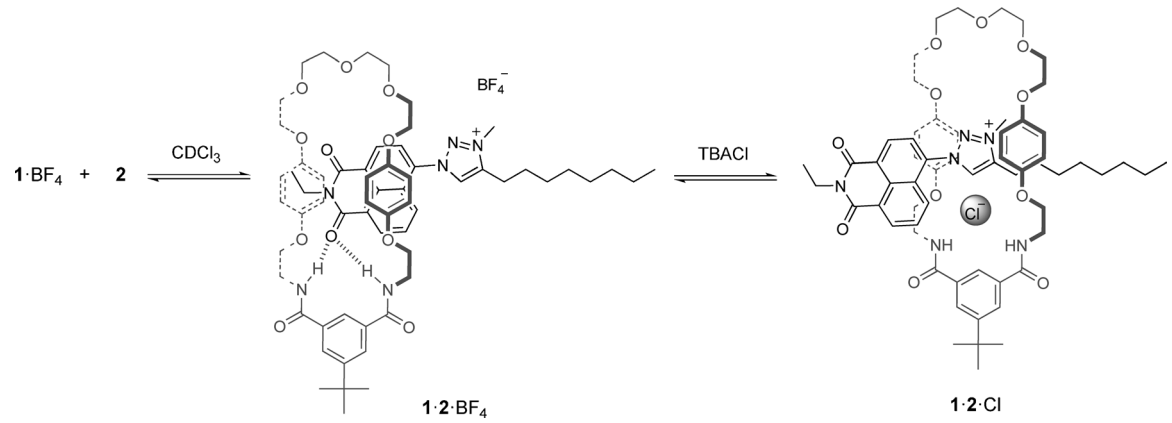

Scheme 1. Formation of pseudorotaxane **1·2**·BF_4 and anion-induced change in co-conformation.

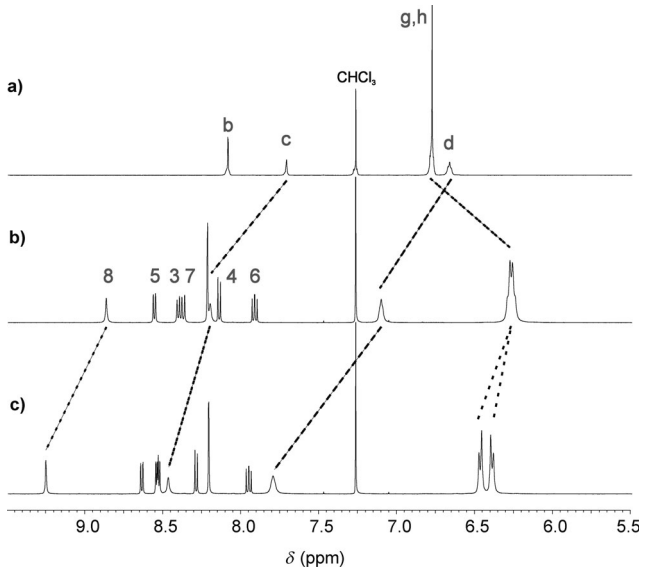

Figure 3. Partial ^{1}H NMR spectra (500 MHz) in $CDCl_3$ at 293 K of a) macrocycle **2**, b) **2** plus 1.0 equivalent of thread **1**·BF_4 and c) **1**·**2**·BF_4 plus 1.0 equivalent of TBACl.

for **1**·**2**·BF_4 and 804(20) M^{-1} for **1**·**2**·Cl. Thus, the two pseudorotaxane assemblies exhibit similar thermodynamic stabilities compared with the respective threading components, **1**·BF_4 and **1**·Cl. However, any comparison is complicated by the fact that strictly the latter value is an apparent 1:1 stability constant for a ternary complex. The pseudorotaxane stability constant for **1**·**2**·BF_4, with the non-coordinating tetrafluoroborate anion, reflects the strength of intercomponent naphthalimide–hydroquinone donor–acceptor and imide–amide hydrogen-bonding interactions present in this assembly. In contrast, the apparent 1:1 stability constant for **1**·**2**·Cl represents only the intercomponent triazolium–hydroquinone donor–acceptor and macrocycle–halide hydrogen-bonding contributions, and does not take into account the electrostatic and hydrogen-bonding interactions between the triazolium thread and the chloride anion, also present in **1**·Cl. However, the triazolium–halide interaction is highly favourable in this non-competitive solvent mixture, both in **1**·Cl and **1**·**2**·Cl, and thus can be said to drive the anion-induced co-conformational change exhibited by **1**·**2**·BF_4 upon the addition of TBACl in $CDCl_3$ (Scheme 1 and Figure 3).

Attempts were made to study both the formation and co-conformations of the pseudorotaxane assemblies with UV/Vis spectroscopy in $CHCl_3$. These titration experiments were undertaken at the same concentration as the ^{1}H NMR experiments (1×10^{-3} M) to avoid the need for large excesses of either component, both of which are UV active. Upon addition of macrocycle **2** to thread **1**·BF_4, the appearance and increase in macrocycle absorbance (290 nm, see the Supporting Information, Figure S14) was accompanied by a decrease in absorption and a slight bathochromic shift in the naphthalimide triazolium band (Figure 4). The donor–acceptor interactions between the macrocycle hydroquinone groups and the naphthalimide triazolium thread are responsible for the pseudorotaxane assembly and result in significant perturbations in the UV/Vis spectra.

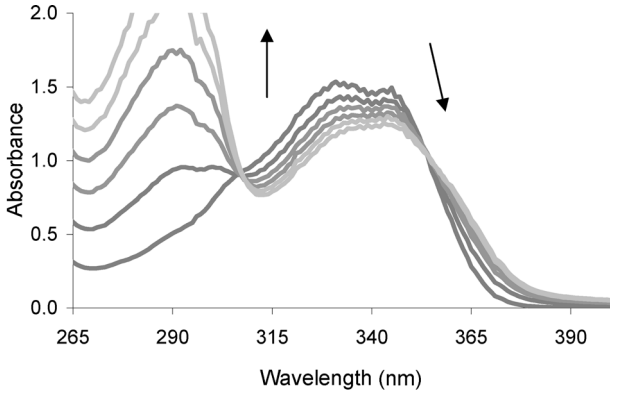

Figure 4. UV/Vis spectra in $CHCl_3$ at 293 K of thread **1**·BF_4 (1.0×10^{-3} M) upon addition of 0.0, 1.0, 2.0, 3.0, 4.0 and 5.0 equivalents of macrocycle **2**.

To investigate whether changes in the pseudorotaxane co-conformation could also be observed by UV/Vis spectroscopy, the effect of chloride addition to solutions of **1**·BF_4 and **2** was studied. However, no changes in absorbance were observed (see the Supporting Information, Figure S15).

In summary, the naphthalimide triazolium threading motifs **1**·BF_4 and **1**·Cl were observed to form pseudorotaxane assemblies with macrocycle **2** of different co-conformations in the presence and absence of a coordinating halide anion. Pseudorotaxane formation was signalled by significant changes in the absorbance band of the naphthalimide triazolium thread, whilst changes in the anion-dependent co-conformation of the interpenetrative assembly were not detectable by UV/Vis spectroscopy.

Rotaxane synthesis: The construction of an interlocked rotaxane structure, incorporating the naphthalimide triazolium motif, was undertaken with the expectation that this system would be capable of undergoing anion-induced molecular motion.

Asymmetric axle component **3**·X (Figure 5) was prepared as detailed in the Supporting Information (Scheme S2), and a "clipping" method was employed for rotaxane formation by using Grubbs'-catalysed ring-closing metathesis (RCM) of bis vinyl-appended macrocycle precursor **4**.[12] Anion templation required the presence of a coordinating anion, and reaction of **3**·Cl with 1.5 equivalents of **4** in dry CH_2Cl_2 with Grubbs' second-generation RCM catalyst afforded the target rotaxane **5**·PF_6 (Scheme 2), isolated in 47% yield, following anion exchange to the non-coordinating hexafluorophosphate salt and purification by preparative silica gel thin-layer chromatography.

The ^{1}H NMR spectrum of rotaxane **5**·PF_6, along with the spectra of axle **3**·BF_4 and macrocycle precursor **4**, is shown in Figure 6. Upon rotaxane formation, the signals associated with the hydroquinone environments f and g move significantly upfield ($\Delta\delta=-0.92$ ppm) due to the expected donor–acceptor interactions. This shift is consistent with the pro-

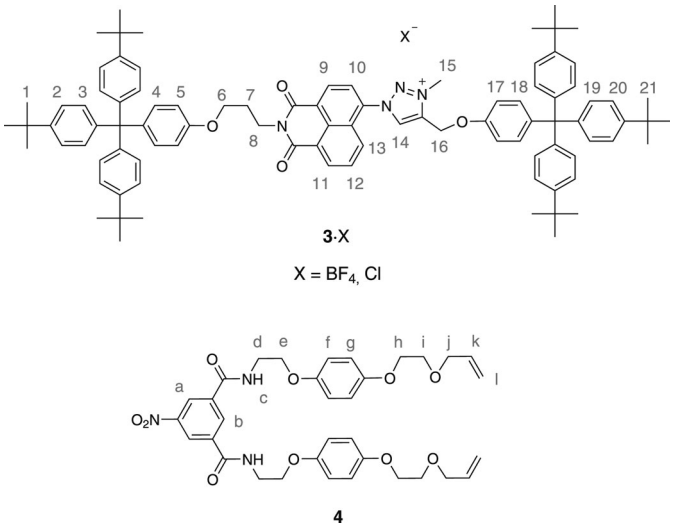

Figure 5. Axle component **3**·X and macrocycle precursor **4** used in rotaxane formation.

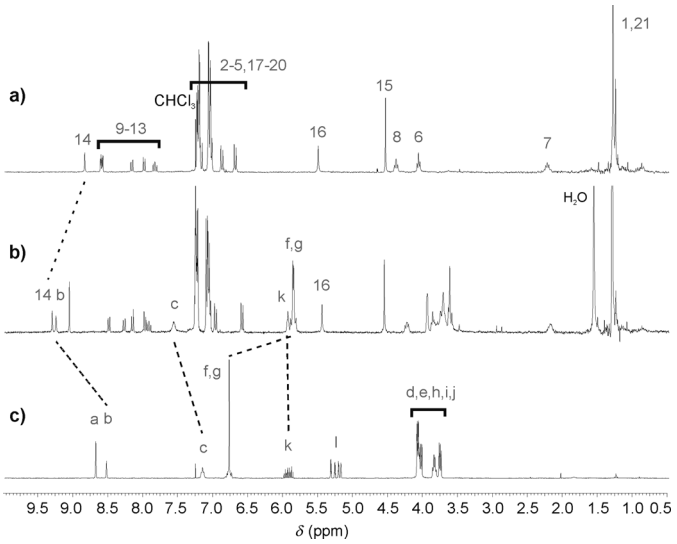

Figure 6. ^{1}H NMR spectra (300 MHz) in $CDCl_3$ at 293 K of a) axle **3**·BF_4, b) rotaxane **5**·PF_6 and c) macrocycle precursor **4**.

posed co-conformation of **5**·PF_6, based on that observed for pseudorotaxane **1**·**2**·BF_4. In addition, macrocycle protons b and c shifted downfield, presumably due to hydrogen-bonding interactions with the axle imide group, along with axle triazolium proton 14.

Further characterisation of rotaxane **5**·PF_6 was provided by high-resolution mass spectrometry and 2D ^{1}H NMR ROESY spectroscopy, with the proposed co-conformation supported by the observed intercomponent ROESY couplings. The spectrum and couplings are shown in the Supporting Information (Figure S6).

Importantly, rotaxane formation was also attempted in the absence of the coordinating halide counter anion by using axle **3**·BF_4, however no rotaxane product was observed in the reaction mixture. This may be rationalised when taking into account that the formation of the analogous pseudorotaxane assembly, **1**·**2**·BF_4, is driven by the donor–acceptor interactions between the macrocycle hydroquinone and axle naphthalimide groups. The pre-organisation of the hydroquinone groups necessary for this association to occur does not exist in macrocycle precursor **4** and is only created in the RCM reaction. Therefore, the synthesis of rotaxane **5**·PF_6 requires the presence of a chloride anion, which successfully templates the association of the two components prior to macrocycle formation. The templation occurs by virtue of halide anion binding interactions with the triazolium and isophthalamide motifs of the axle and macrocycle precursor.

Rotaxane NMR studies—shuttling: ^{1}H NMR spectroscopy was used to investigate the chloride-anion-induced co-conformational behaviour of rotaxane **5**·PF_6 (Scheme 3).

The ^{1}H NMR spectrum of rotaxane **5**·PF_6 in $CDCl_3$ is shown in Figure 7a, along with the spectrum observed after addition of one equivalent of TBACl (Figure 7b). Downfield shifts in protons 14, b, c, f and g were observed, as well as a significant upfield shift in the signal corresponding to axle protons 16. The downfield shifts in protons 14, b and c indicate cooperative hydrogen bonding to the chloride anion by the macrocycle isophthalamide and axle triazolium binding

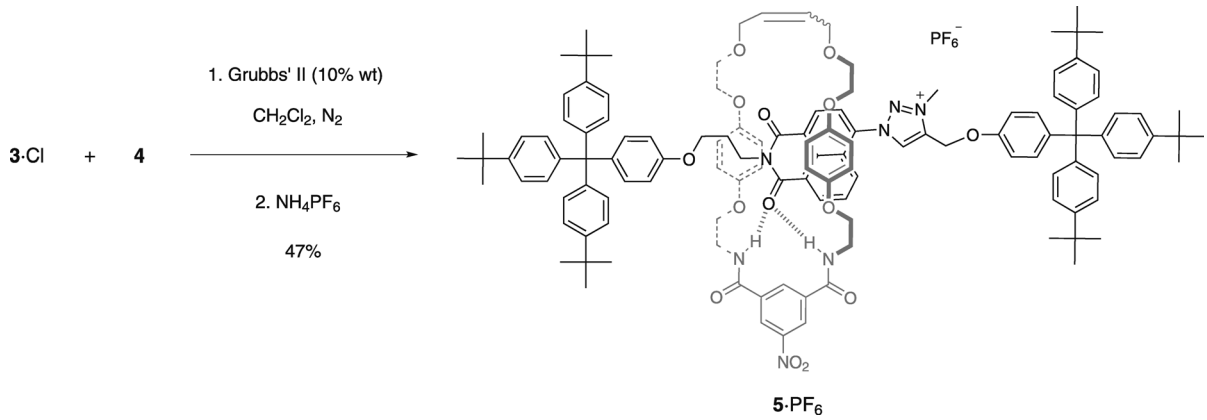

Scheme 2. Synthesis of naphthalimide triazolium rotaxane **5**·PF_6.

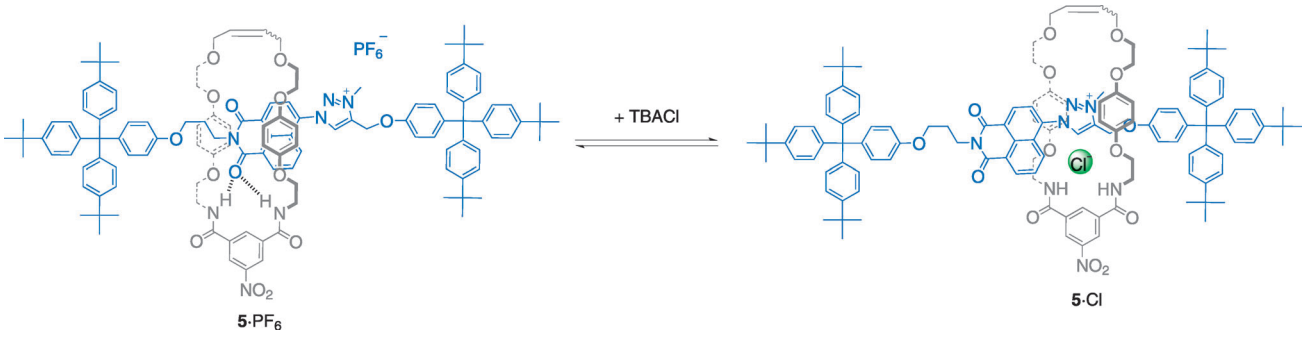

Scheme 3. Anion-induced molecular shuttling exhibited by rotaxane **5**·PF_6.

motifs. The creation of a unique anion-binding cavity within the rotaxane requires macrocycle translocation (Scheme 3), and the different extents of shielding associated with the two rotaxane co-conformations are reflected in the shifts observed for protons f, g and 16. The macrocycle hydroquinone protons experience a greater shielding effect when they reside over the naphthalimide group of the axle in the starting co-conformation (**5**·PF_6), compared with over the triazolium group in **5**·Cl. This reduction in shielding results in a downfield shift of macrocycle hydroquinone protons f and g after the addition of TBACl (Figure 7b), and is similar to that observed between pseudorotaxane co-conformations **1**·**2**·BF_4 and **1**·**2**·Cl (Figure 3). Moreover, when the macrocycle resides over the triazolium group, axle CH_2 protons 16 become partially shielded by the hydroquinone groups. This shielding effect is not present in **5**·PF_6, thus an upfield shift in the signal corresponding to protons 16 is observed upon halide anion addition.[13]

Crystals suitable for single-crystal X-ray diffraction structural determination of rotaxane **5**·Cl were analysed by using synchrotron radiation at Diamond Light Source beamline I19.[14] The co-conformation of the interlocked structure in the solid state is in agreement with that proposed for the solution phase, namely, with the macrocycle hydroquinone groups residing over the axle triazolium group (Figure 8). Importantly, the chloride anion is bound within the rotaxane-host cavity by hydrogen-bonding interactions to protons b, c, 14 and 16 ($C-H^{b}\cdots Cl^-$ distance 3.348(9) Å, $N-H^{c}\cdots Cl^-$ 3.218(8) Å, $N-H^{c'}\cdots Cl^-$ 3.297(8) Å, $C-H^{14}\cdots Cl^-$ 3.309(6) Å and $C-H^{16}\cdots Cl^-$ 3.391(6) Å). Further examination of the crystalline network reveals that the naphthalimide group of the axle component is involved in π-donor–π-acceptor interactions with a hydroquinone group of an adjacent rotaxane molecule (centroid-to-centroid distance 3.471(4) Å, ring dihedral angle 8.3(3)°; see the Supporting Information, Figure S19). This illustrates the potential for this interaction, with the analogous intercomponent donor–acceptor interactions responsible for the proposed solution-phase co-conformation of **5**·PF_6.

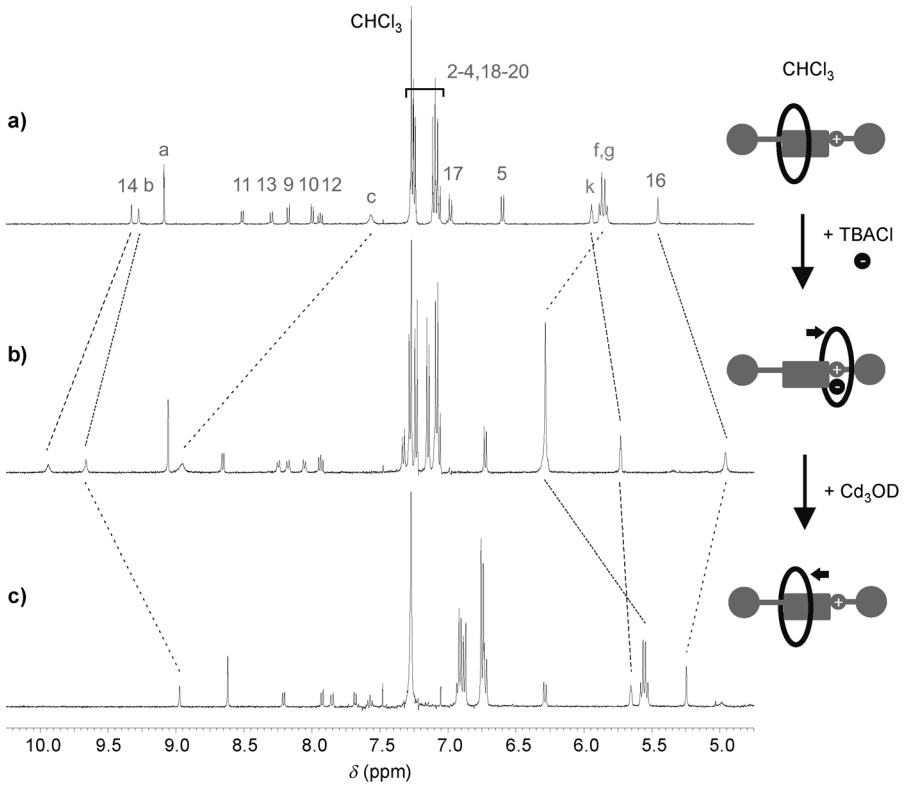

Figure 7. Partial ^{1}H NMR spectra (500 MHz) at 293 K of a) rotaxane **5**·PF_6 in $CDCl_3$, b) rotaxane **5**·PF_6 plus 1.0 equivalent of TBACl in $CDCl_3$ and c) rotaxane **5**·PF_6 + 1.0 equivalent of TBACl in 1:1 $CDCl_3/CD_3OD$.

On account of the change in rotaxane co-conformation being driven by the hydrogen-bonding interactions between the isophthalamide and triazolium groups of **5**·PF_6 and the coordinated chloride anion, increasing the competitive nature of the solvent through protic-solvent addition should weaken these interactions and eventually reverse the molecular-motion

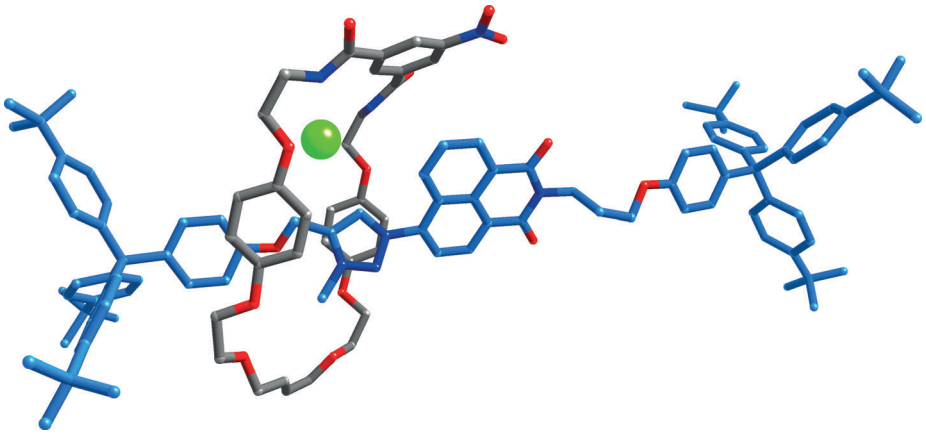

Figure 8. Crystal structure of rotaxane **5**·Cl. Protons and lower-occupancy positions of disorder are omitted for clarity.

shuttling process. Upon addition of increasing amounts of CD_3OD to a $CDCl_3$ solution of **5**·Cl, ^1H NMR shifts were observed to indicate that macrocycle translocation back to the initial co-conformation was indeed occurring; the spectrum for 1:1 $CDCl_3/CD_3OD$ is shown in Figure 7c. The loss of the halide anion from the rotaxane binding cavity is reflected in an upfield shift in isophthalamide proton b (the signals corresponding to triazolium proton 14 and amide protons c were not observed after CD_3OD addition due to deuterium exchange). The return to the starting co-conformation, and the associated changes in the shielding effects, are shown by an upfield shift in hydroquinone protons f and g and a downfield shift in axle protons 16—the reverse of the shifts observed upon chloride anion addition to **5**·PF_6 in $CDCl_3$ (Figure 7b).

The change in rotaxane co-conformation can be monitored by following the relative positions of the macrocycle hydroquinone and alkene proton signals throughout the halide and CD_3OD NMR titration experiments (Figure 9). The gradual changes in the relative positions of these peaks indicate that the molecular motion exhibited by rotaxane **5**·PF_6 is a dynamic process, which is fast on the NMR timescale. The shuttling behaviour is reversible and, importantly, can be controlled by dual stimulus, namely, halide anion addition followed by an increase in the competitive nature of the solvent.

The anion-induced co-conformational change exhibited by naphthalimide triazolium rotaxane was further supported by 2D ^1H NMR ROESY spectroscopy, with the proposed solution-phase co-conformation of **5**·Cl confirmed by the observed intercomponent couplings (see the Supporting Information, Figure S7).

Rotaxane NMR studies—anion binding: The anion-binding properties of rotaxane **5**·PF_6 with a range of TBA anion salts, that is, chloride, bromide, iodide, dihydrogen phosphate and acetate, were investigated by ^1H NMR titration experiments. Binding was too strong for accurate association-constant values to be determined in $CDCl_3$, so the more competitive 4:1 $CDCl_3/CD_3OD$ solvent mixture was used.[15]

Downfield shifts for the axle triazolium and macrocycle isophthalamide C–H protons (14 and b) and macrocycle amide N–H protons (c) of the rotaxane were observed upon addition of TBACl to **5**·PF_6 in these solvent conditions (Figure 10). It was not possible to follow the triazolium and amide protons (14 and c) throughout the titration due to deuterium exchange. Additional shifts occurred for the signals corresponding to protons 16, f, g and k, due to the same shielding effects discussed above and seen in Figure 7.

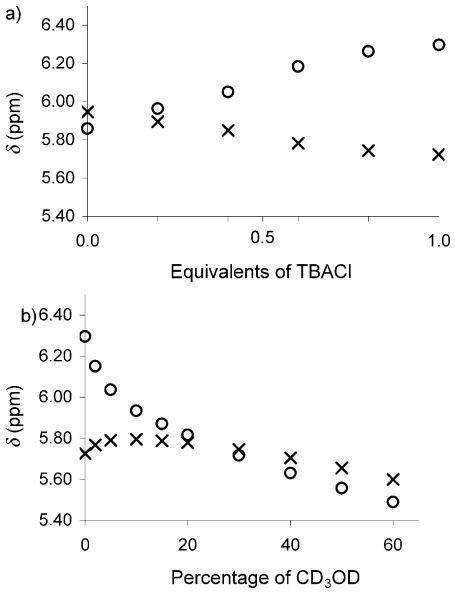

Figure 9. Changes in the chemical shift of alkene protons k (×) and hydroquinone protons f and g (○) in rotaxane **5**·PF_6 in $CDCl_3$ at 293 K upon a) addition of TBACl, and b) subsequent addition of CD_3OD.

During the titration experiments for the other anions (bromide, iodide, acetate and dihydrogen phosphate), downfield shifts in isophthalamide and amide anion binding protons b and c were observed as expected, however, triazolium proton 14 exhibited anion-dependent differential behaviour. Before deuterium exchange, this proton signal shifted downfield upon addition of chloride and dihydrogen phosphate, and slightly upfield with iodide addition, whereas no significant shifts were observed upon bromide and acetate addition (Figure S10 in the Supporting Information). These contrasting observations are thought to be the consequence of the combination of downfield and upfield perturbations, re-

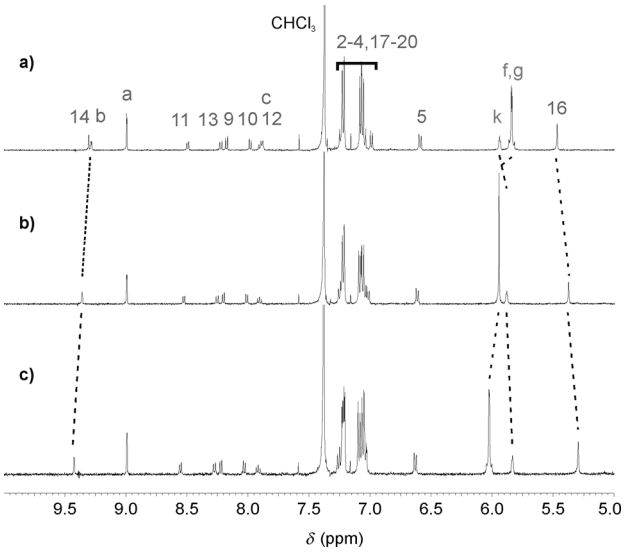

Figure 10. Partial ^{1}H NMR spectra (500 MHz) in 4:1 $CDCl_3/CD_3OD$ at 293 K of a) rotaxane **5**·PF_6, b) rotaxane **5**·PF_6 plus 1.0 equivalent of TBACl and c) rotaxane **5**·PF_6 plus 5.0 equivalents of TBACl.

sulting from hydrogen-bonding interactions with the anion and increased shielding from the hydroquinone groups upon macrocycle translocation. The relative magnitudes of these effects are likely to be dependent on the nature of the anion, relating to the basicity of the anion and any differences in the exact co-conformation of the rotaxane-host structure.

By using WinEQNMR2,[11] 1:1 stoichiometric association constants were determined from the titration data by monitoring macrocycle isophthalamide proton b of the rotaxane host (Table 1). This proton is directly involved in anion binding and could be accurately monitored throughout all titration experiments.

Table 1. Association constants, K [M^{-1}], of rotaxane **5**·PF_6 with anions in 4:1 $CDCl_3/CD_3OD$ at 293 K. Obtained by monitoring proton b. Errors are given in brackets.

Anion	Cl^-	Br^-	I^-	$H_2PO_4^-$	OAc^-
K [M^{-1}]	527 (47)	673 (7)	173 (17)	83 (6)	59 (1)

Table 1 shows that the smaller halide anions, that is, chloride and bromide, are bound considerably more strongly than the larger iodide and more basic oxoanions, dihydrogen phosphate and acetate. This is due to the three-dimensional anion-binding cavity created within the interlocked structure upon co-conformational change, which is of complementary size and shape for the smaller halide guest species, with bromide bound slightly more strongly than chloride.

The possibility of a different binding mode, external to the rotaxane cavity, for the larger anions (iodide, dihydrogen phosphate and acetate) is supported by differential shifts observed for axle CH_2 protons 16 during the titration experiments (see the Supporting Information, Figure S11). These protons shifted significantly upfield upon addition of chloride and bromide ($\Delta\delta = -0.19$ and -0.16 ppm, respectively, after 10.0 equivalents), assigned to increased shielding from hydroquinone groups upon macrocycle translocation. In contrast, very slight downfield shifts of 0.02–0.05 ppm occurred with the larger anions, indicating that any alteration in the relative position of the macrocycle upon addition of iodide and the oxoanions is not sufficient to perturb these protons.

Some change in the co-conformation of the rotaxane-host **5**·PF_6 is necessary for all of the anions to interact with both axle and macrocycle C-H and amide N-H hydrogen bond donor anion binding motifs, however these ^{1}H NMR shifts indicate that complete macrocycle translocation from the naphthalimide group of the axle to the triazolium group (as seen in the solid state, Figure 8) only occurs with the strongly bound chloride and bromide anions. The larger anions are not able to bind within the rotaxane-host cavity, resulting in weaker external binding and a reduction in the extent of macrocycle translocation, presumably to retain some of the favourable naphthalimide–hydroquinone donor–acceptor interactions. This potential selectivity is also supported by the behaviour of hydroquinone and alkene protons (f, g and k) during the titrations (see the Supporting Information, Figure S12 and Table S1). Considerably smaller perturbations were observed with iodide, dihydrogen phosphate and acetate than with chloride and bromide, again indicating that the extent of co-conformational change is much less with the weaker-bound anions.

Rotaxane UV/Vis studies: Having quantified the selectivity in the anion-induced shuttling of rotaxane **5**·PF_6 with ^{1}H NMR titration experiments, we then investigated whether the change in the interlocked co-conformation could be detected by UV/Vis spectroscopy. The magnitude of any such response to different anions and the reversibility of the molecular motion were studied in the less-competitive solvent $CHCl_3$, to ensure saturation in binding, and the associated co-conformational changes, but after the addition of only several equivalents of anion.

Naphthalimide triazolium axle **3**·BF_4 did not display any perturbations in its UV/Vis spectrum upon addition of anions in $CHCl_3$ (see the Supporting Information, Figure S16). However, the addition of TBACl to rotaxane **5**·PF_6 yielded a slight hypsochromic shift of the naphthalimide absorbance band, along with an enhancement in absorption (Figure 11a). These gradual changes were observed upon addition of up to two equivalents of chloride, after which the UV/Vis spectra remained unchanged. Hence, the relative position of the macrocycle within the rotaxane-host structure does indeed affect the naphthalimide absorbance band, presumably due to changes in the donor–acceptor interactions present in the two co-conformations. It is thought that macrocycle translocation is signalled effectively, in contrast to the pseudorotaxane assemblies, due to the interlocked nature of rotaxane **5**·PF_6.

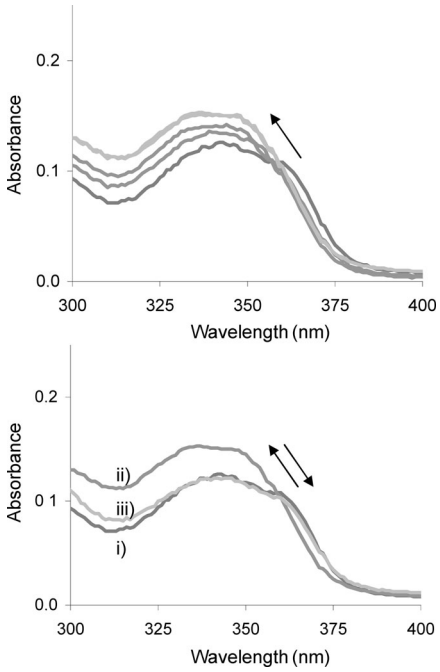

Figure 11. UV/Vis spectra of a) rotaxane **5**·PF_6 upon addition of 0.0, 0.5, 1.0, 2.0 and 5.0 equivalents of TBACl; b) i) rotaxane **5**·PF_6, ii) after addition of 5.0 equivalents of TBACl and iii) after subsequent addition of $AgPF_6$ and filtration. All spectra were recorded in $CHCl_3$ at 293 K, $c = 1.0 \times 10^{-5}$ M.

Similar perturbations were also observed upon addition of bromide, iodide and dihydrogen phosphate to rotaxane **5**·PF_6 (see the Supporting Information, Figure S17).[16] With chloride and bromide, increases in absorbance at 340 nm of 15 and 16% were observed after saturation, whilst dihydrogen phosphate addition resulted in a considerably smaller change of 6%. This indicates that the reduced extent of macrocycle translocation with the larger oxoanion is reflected directly in the UV/Vis response to dihydrogen phosphate. However, complete macrocycle translocation was not observed for iodide either in the ^{1}H NMR studies, but this was not evident in the UV/Vis investigations (14% increase in absorbance).

To investigate whether the reversibility of this shuttling behaviour could be demonstrated, a large excess of $AgPF_6$ was added to a solution of rotaxane **5**·PF_6 in the presence of five equivalents of TBACl. Importantly, the naphthalimide absorbance band shifted back to its initial position (Figure 11b), indicating a return to the original co-conformation.

In summary, perturbations of the naphthalimide axle absorbance band—due to co-conformational-dependent π-donor–π-acceptor interactions with the macrocycle hydroquinone groups—enabled the reversible, anion-induced shuttling exhibited by rotaxane-host-structure **5**·PF_6 to be signalled and monitored by UV/Vis spectroscopy.[17]

Conclusion

By exploiting the naphthalimide triazolium motif, a novel rotaxane host system was prepared by using chloride-anion templation and demonstrated to exhibit selective, uni-directional, anion-induced shuttling as evidenced by ^{1}H NMR and UV/Vis spectroscopy.

Initial ^{1}H NMR pseudorotaxane investigations between tetrafluoroborate and chloride thread salts and an isophthalamide-containing macrocycle revealed the ability of the naphthalimide triazolium motif to form interpenetrated assemblies with counter-anion-dependent co-conformations.

The uni-directional shuttling behaviour of the analogous rotaxane was driven by anion binding and controlled by the dual stimulus of anion addition and by increasing the competitive nature of the solvent. ^{1}H NMR titration experiments revealed selectivity in rotaxane-host binding, and the extent of macrocycle translocation was observed to be anion dependent. Complete macrocycle translocation only occurred upon the recognition of the strongly bound smaller halide anions, namely, chloride and bromide. The three-dimensional anion-binding cavity of the rotaxane, which results upon co-conformational change, is responsible for this selectivity. The solid-state crystal structure of the rotaxane in the presence of chloride supports the proposed solution-phase co-conformational behaviour.

Changes in the co-conformation of the rotaxane upon anion addition were detected by UV/Vis spectroscopy due to the sensitivity of the axle naphthalimide absorbance band to the position of the macrocycle component within the interlocked structure. The chloride-induced shuttling behaviour of the rotaxane was demonstrated to be reversible upon addition of silver hexafluorophosphate.

Experimental Section

General considerations: Commercially available solvents and chemicals were used without further purification, unless otherwise stated. Dry solvents were obtained by purging with nitrogen and then passing through an MBraun MPSP-800 column. Water was de-ionised and micro-filtered with a Milli-Q ® Millipore machine. All tetrabutylammonium salts and Grubbs' second-generation catalyst were stored in a vacuum desiccator prior to use.

NMR spectra were recorded on Varian Mercury 300, Varian Unity Plus 500 and Bruker AVII 500 (with ^{13}C Cryoprobe) spectrometers. Mass spectrometry was carried out on a Bruker micrOTOF spectrometer. Melting points were recorded on a Gallenkamp capillary melting point apparatus and are uncorrected.

Literature procedures were used in the preparations of **2**[10] and **4**.[12] The syntheses of **1**·BF_4, **1**·Cl, **3**·BF_4 and **3**·Cl are given in the Supporting Information.

Rotaxane 5·PF_6: Axle **3**·Cl (40 mg, 0.029 mmol) and macrocycle precursor **4** (28 mg, 0.044 mmol) were dissolved in dry CH_2Cl_2 (10 mL) and stirred for 30 min. Grubbs' second-generation catalyst (10% by weight, 2.8 mg) was then added and the reaction mixture was left to stir at room temperature for 15 h under N_2. The solvent was removed in vacuo and macrocyclic byproducts removed by preparative silica gel thin-layer chromatography (6:4 CH_2Cl_2/CH_3CN). The crude product and unreacted **3**·Cl were dissolved in CH_2Cl_2 (20 mL) and washed with 0.1 M NH_4PF_6 (aq)

(10×10 mL) and water (4×10 mL). The organic fraction was dried over $MgSO_4$ and in vacuo, and the residue purified by preparative silica gel thin-layer chromatography (4% CH_3OH/CH_2Cl_2) to yield **5**·PF_6 as a yellow solid (29 mg, 0.014 mmol, 47%). M.p.: 179–181 °C; ^{1}H NMR (500 MHz, $CDCl_3$): δ = 9.30 (s, 1H, H_{14}), 9.26 (apps, 1H, H_b), 9.06 (d, ^4J = 1.3 Hz, 1H, H_a), 8.52 (d, ^3J = 7.3 Hz, 1H, H_{11}), 8.28 (d, ^3J = 8.5 Hz, 1H, H_{13}), 8.18 (d, ^3J = 7.9 Hz, 1H, H_9), 7.99 (d, ^3J = 7.9 Hz, 1H, H_{10}), 7.93 (dd, ^3J = 8.5 Hz, ^3J = 7.3 Hz, 1H, H_{12}), 7.58 (brs, 2H, c), 7.22–7.27 (m, 12H, H_2 and H_{20}), 7.05–7.12 (m, 16H, H_3, H_4, H_{18} and H_{19}), 6.98 (d, ^3J = 8.8 Hz, 2H, H_{17}), 6.61 (d, ^3J = 8.8 Hz, 2H, H_5), 5.92–5.98 (m, 2H, H_k), 5.80–5.91 (m, 8H, H_f and H_g), 5.47 (s, 2H, H_{16}), 4.58 (s, 3H, H_{15}), 4.21–4.27 (m, ^3J = 7.0 Hz, 2H, H_8), 3.95 (brs, 4H, H_j), 3.86–3.89 (m, 2H, H_6), 3.59–3.85 (m, 16H, H_d, H_e, H_h and H_i), 2.16–2.23 (m, 2H,H_7), 1.32 (s, 27H, H_1 or H_{21}), 1.31 ppm (s, 27H, H_1 or H_{21}); ^{19}F NMR (282.5 MHz, $CDCl_3$): δ = −73.4 ppm (d, ^1J = 712 Hz, PF_6); ^{13}C NMR (125 MHz, $CDCl_3$): δ = 165.8, 164.9, 162.6, 156.3, 154.7, 152.0, 151.6, 149.2, 148.6, 148.3, 144.1, 143.7, 142.4, 140.4, 140.2, 136.0, 133.9, 132.9, 132.8, 132.3, 131.3, 130.8, 130.7, 130.6, 129.6, 129.5, 129.4, 128.8, 127.5, 126.7, 125.6, 125.2, 124.2, 124.1, 122.2, 114.2, 113.9, 113.1, 112.9, 70.7, 69.5, 67.1, 66.9, 65.4, 63.1, 63.0, 58.3, 40.9, 39.2, 38.8, 34.3, 34.3, 31.4, 31.4, 28.0 ppm; HRMS (ESI): *m/z*: calcd for $C_{125}H_{138}N_7O_{14}$: 1962.0329 $[M-PF_6]^+$; found: 1962.0347 .

Acknowledgements

G.T.S. thanks the EPSRC for a studentship (EP/F011504) and Nicholas G. White for help with crystallography. M.B.P. thanks the Diamond Light Source (U.K.) for synchrotron beam time on I-19 and the (EPSRC) National Crystallography Service for data collection.

[1] A. Coskun, M. Banaszak, R. D. Astumian, J. F. Stoddart, B. A. Grzybowski, *Chem. Soc. Rev.* **2012**, *41*, 19–30; V. Balzani, A. Credi, M. Venturi, *Molecular Devices and Machines: Concepts and Perspectives for the Nanoworld*, Wiley, Weinheim, **2008**; E. R. Kay, D. A. Leigh, F. Zerbetto, *Angew. Chem.* **2007**, *119*, 72–196; *Angew. Chem. Int. Ed.* **2007**, *46*, 72–191; V. Balzani, A. Credi, S. Silvi, M. Venturi, *Chem. Soc. Rev.* **2006**, *35*, 1135–1149; *Structure and Bonding, Vol 99: Molecular Machines and Motors* (Ed.: J. P. Sauvage), Springer, Berlin Heidelberg, **2001**.

[2] P. A. Gale, T. Gunnlaugsson, *Chem. Soc. Rev.* **2010**, *39*, 3595–3596.

[3] E. V. Dzyuba, L. Kaufmann, N. L. Löw, A. K. Meyer, H. D. F. Winkler, K. Rissanen, C. A. Schalley, *Org. Lett.* **2011**, *13*, 4838–4841; C. J. Serpell, R. Chall, A. L. Thompson, P. D. Beer, *Dalton Trans.* **2011**, *40*, 12052–12055; N. H. Evans, C. J. Serpell, P. D. Beer, *Chem. Eur. J.* **2011**, *17*, 7734–7738; T.-C. Lin, C.-C. Lai, S.-H. Chiu, *Org. Lett.* **2009**, *11*, 613–616; M. J. Barrell, D. A. Leigh, P. J. Lusby, A. M. Z. Slawin, *Angew. Chem.* **2008**, *120*, 8156–8159; *Angew. Chem. Int. Ed.* **2008**, *47*, 8036–8039; C.-F. Lin, C.-C. Lai, Y.-H. Liu, S.-M. Peng, S.-H. Chiu, *Chem. Eur. J.* **2007**, *13*, 4350–4355; Y.-L. Huang, W.-C. Hung, C.-C. Lai, Y.-H. Liu, S.-M. Peng, S.-H. Chiu, *Angew. Chem.* **2007**, *119*, 6749–6753; *Angew. Chem. Int. Ed.* **2007**, *46*, 6629–6633.

[4] J. J. Gassensmith, S. Matthys, J.-J. Lee, A. Wojcik, P. V. Kamat, B. D. Smith, *Chem. Eur. J.* **2010**, *16*, 2916–2921.

[5] H. Zheng, W. Zhou, J. Lv, X. Yin, Y. Li, H. Liu, Y. Li, *Chem. Eur. J.* **2009**, *15*, 13253–13262.

[6] B. W. Laursen, S. Nygaard, J. O. Jeppesen, J. F. Stoddart, *Org. Lett.* **2004**, *6*, 4167–4170.

[7] A. M. Brouwer, C. Frochot, F. G. Gatti, D. A. Leigh, L. Mottier, F. Paolucci, S. Roffia, G. W. H. Wurpel, *Science* **2001**, *291*, 2124–2128.

[8] M. D. Lankshear, P. D. Beer, *Acc. Chem. Res.* **2007**, *40*, 657–668.

[9] K. M. Mullen, J. Mercurio, C. J. Serpell, P. D. Beer, *Angew. Chem.* **2009**, *121*, 4875–4878; *Angew. Chem. Int. Ed.* **2009**, *48*, 4781–4784.

[10] M. R. Sambrook, P. D. Beer, J. A. Wisner, R. L. Paul, A. R. Cowley, F. Szemes, M. G. B. Drew, *J. Am. Chem. Soc.* **2005**, *127*, 2292–2302.

[11] M. J. Hynes, *J. Chem. Soc. Dalton Trans.* **1993**, 311–312.

[12] M. R. Sambrook, P. D. Beer, M. D. Lankshear, R. F. Ludlow, J. A. Wisner, *Org. Biomol. Chem.* **2006**, *4*, 1529–1538.

[13] Only minimal shifts in the axle naphthalimide protons of **5**·PF_6 were observed upon chloride addition, indicating no significant interactions between these protons and the halide anion.

[14] Crystal data for **5**·Cl: formula: $C_{93}H_{103}N_4O_4{\cdot}C_{32}H_{35}N_3O_{10}{\cdot}Cl$, M = 1997.87, monoclinic, $P2_1/c$ (no. 14), a = 11.519(6), b = 14.600(7), c = 73.86(4) Å, β = 90.161(7)°, V = 12422(11) Å^3, Z = 4, ρ_{calcd} = 1.068 g cm^{-3}, μ = 0.090 mm^{-1}, T = 100 K, colourless plate (0.10×0.04×0.01 mm^3), Crystal Logic diffractometer and Rigaku Saturn 724+ detector (λ = 0.68890 Å, Diamond Light Source, I-19 beamline); 19476 independent measured reflections (R_{int} = 0.1266), F^2 refinement, final R_1 ($F^2 > 2\sigma(F^2)$) = 0.1006, $wR_2(F^2 > 2\sigma(F^2))$ = 0.2518, GoF = 0.907, data completeness to θ = 24.21° = 88.7%. CCDC-862707 contains the supplementary crystallographic data for this paper. These data can be obtained free of charge from The Cambridge Crystallographic Data Centre via www.ccdc.cam.ac.uk/data_request/cif.

[15] Anion binding did not occur in the more competitive 1:1 $CDCl_3$/CD_3OD solvent mixture, which was used for the triazolium rotaxane in ref. [9], presumably due to the extra energetic cost of macrocycle translocation in **5**·PF_6.

[16] Due to the insolubility of TBAOAc in $CHCl_3$, the response upon acetate addition was could not be investigated.

[17] We also intended to investigate the fluorescence of this system. However, rotaxane **5**·PF_6 was barely fluorescent, displayed excitation-dependent emission and produced very minor, irreproducible responses to anions. It is thought that this is due to quenching effects from the macrocycle, as well as potentially complicating twisted internal charge transfer (TICT) behaviour (J. R. Lakowicz, *Principles of Fluorescence Spectroscopy*, 3rd ed., Springer, New York, **2006**).

Received: January 30, 2012
Published online: ■■ ■■, 0000

Molecular Motion

*G. T. Spence, M. B. Pitak, P. D. Beer**..... ▮▮▮▮–▮▮▮▮

Anion-Induced Shuttling of a Naphthalimide Triazolium Rotaxane

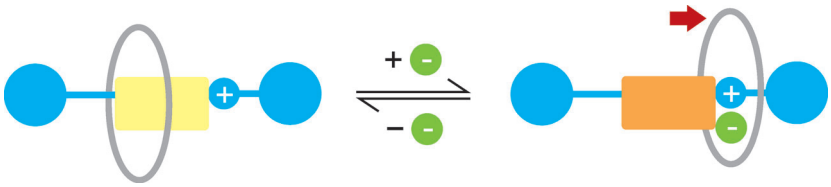

Selective shuttling: The anion-templated synthesis of a rotaxane structure, incorporating the novel naphthalimide triazolium motif, is described and the interlocked host shown to exhibit selective, uni-directional, anion-induced shuttling behaviour (see scheme), as evidenced by ^{1}H NMR and UV spectroscopy.